JVSTA
Journal of Vacuum Science & Technology A

Growth behavior and interfacial reaction between carbon nanotubes and Si substrate

Chih-Ming Hsu, Hong-Jen Lai, and Cheng-Tzu Kuo

Citation: Journal of Vacuum Science & Technology A **22**, 1461 (2004); doi: 10.1116/1.1735908
View online: http://dx.doi.org/10.1116/1.1735908
View Table of Contents: http://scitation.aip.org/content/avs/journal/jvsta/22/4?ver=pdfcov
Published by the AVS: Science & Technology of Materials, Interfaces, and Processing

Growth behavior and interfacial reaction between carbon nanotubes and Si substrate

Chih-Ming Hsu[a)] and Hong-Jen Lai
Industrial Technology Research Institute, Materials Research Laboratories, 195 Sec. 4, Chung Hsing Road, Chutung, Hsinchu 310, Taiwan

Cheng-Tzu Kuo
National Chiao Tung University, Department of Materials Science and Engineering, 1001 Ta-Hsueh Road, Hsinchu 300, Taiwan

(Received 21 October 2003; accepted 8 March 2004; published 20 July 2004)

The effect of the interfacial reaction of Co catalyst with a Si substrate on growth of carbon nanotubes (CNTs) was investigated. Well-aligned multiwall CNTs (MWCNTs) were synthesized and applied barrier layers by microwave plasma-enhanced chemical vapor deposition (MPECVD). Growth proceeded in a flowing mixture of H_2, CH_4, and N_2 as precursors at a temperature of 600 °C and a −200 V substrate bias; Co was sputtered as the catalytic material. Transmission electron microscopy (TEM) and x-ray diffraction were employed to examine the growth behavior of CNTs on Si (100) substrates on which Co had been deposited by MPECVD. The TEM results indicate that discrete conical $CoSi_2$ layers with {111} and (100) faceted interfaces were formed on a Si (100) substrate during CNTs growth. Direct evidence that the growth is by tip growth and base growth is presented. The results show that well-aligned CNTs exhibit a significant emission current. The field emission characteristics of CNTs are contributed to the relationship between the application of different barrier layers and the growth mode of CNTs. © *2004 American Vacuum Society.* [DOI: 10.1116/1.1735908]

I. INTRODUCTION

The identification of the structure of carbon nanotubes (CNTs) by Iijima in 1991[1] was a scientific milestone. CNTs have attracted intense interest in the field of nanotechnology because of their unique properties and wide range of applications, such as nanoelectronics,[2,3] scanning probes, and[4] field emission displays (FEDs).[5,6] The selective growth of CNTs on Si wafers, catalyzed by Fe, Co, Ni, or other elements, is important in the CNTs deposition. However, the metal silicide produced at high temperature in the CVD growth[7–9] and transition-metal silicides are crucial materials for the tremendous success of Si integrated circuits; titanium and cobalt silicide are the two more widely used self-aligned silicides.[10] For this reason, CNTs have potential for use in interconnects in electronic devices, contact windows of silicide and field emitters. However, strong adhesion between CNTs, electron-emitting layers and substrates were required for fabricating practical cold cathodes in applying electron emitting devices. The interaction between metal catalysts and substrate, in growth processes of CNTs presented by several groups,[7–9] can ensure excellent adhesion and field emission properties. This study considers the interfacial reactions among CNTs, cobalt, and the Si substrate. The relationship between interfacial reactions and field emission characteristics on the growth of CNTs is also investigated.

II. EXPERIMENT

CNTs were synthesized on Co (75 nm)-coated Si (100) wafers using microwave plasma-enhanced chemical vapor deposition (MPECVD), in which the Co film was generated by physical vapor deposition. The synthetic process as follows: (1) A 500 W H_2 plasma pretreatment for Co film for 10 min at 9 Torr, formed well-distributed nanosized catalysts; (2) CH_4/N_2 process gases were introduced in a ratio of 10/100 sccm, at a deposition pressure of 16 Torr and a microwave power of 800 W, for 10 min. Interfacial reaction between CNTs and Si substrate were obtained by x-ray diffraction (XRD) to identify crystal phases. Scanning electron microscopy (SEM) was used to characterize the growth morphologies of the CNTs, and the cross sections and microstructures of the CNTs were observed by transmission electron microscopy (TEM); the depth profiles of the catalytic film were obtained by Auger electron spectra (AES). Field emission from the arrays of CNTs and the relationships between the buffer layers were measured in a vacuum chamber equipped with electrical stepper and applied a high voltage between the sample and anode. The typical spacing from the tip of the CNT arrays to the anode is 100 μm. All of the current measurements were taken in a vacuum at a pressure of 10^{-6} Torr with an electrometer (Keithley 237) and recorded by a personal computer.

III. RESULTS AND DISCUSSION

Aligned CNTs were successfully synthesized on a Co-deposited Si substrate. Figure 1(a) shows the typical SEM morphology of CNTs. The figure indicates that aligned but

[a)]Author to whom correspondence should be addressed; electronic mail: jimmyhsu@itri.org.tw

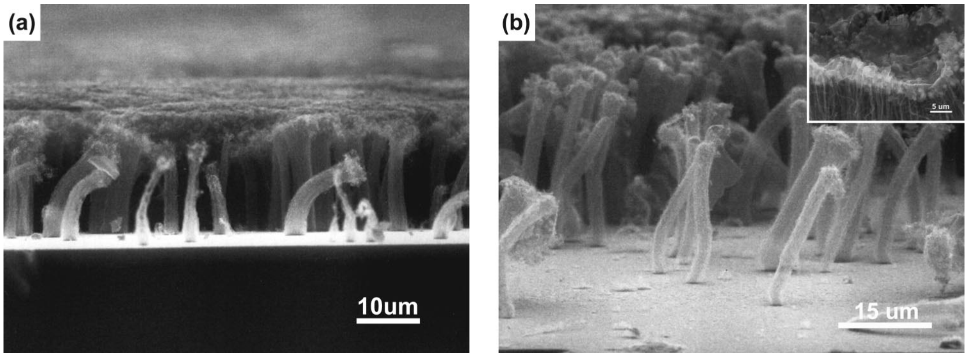

FIG. 1. SEM morphologies of CNTs grown applied a SiO_2 barrier layer: (a) well aligned CNTs cover the substrate; (b) a highly magnified SEM image of the CNTs arrays increases the length with growth time, reaching 10 μm after 10 min.

tangled CNTs cover the substrate. The length of the CNTs arrays increases with growth time, reaching 10 μm after 10 min. A highly magnified SEM image, displayed in Fig. 1(b), depicts CNTs, growing separately and perpendicularly out of the substrate in bundles of CNTs. Observation of the interface between the CNTs and the Si substrate reveals a cross section of the specimen prepared using a diamond saw and polishing. Peeled out CNTs with a collapsed bottom-end are observed in this specimen, shown in Fig. 2(a). CNTs grown by this method should have defects, resulting in crooked and entangled shapes. The SEM image [Fig. 2(b)] of the bottom end of the stripped-out CNT arrays includes more CNTs with distorted and collapsed bottom-ends, corresponding to the continued presence of the cone-shaped Co particles on the Si substrate, as presented in Fig. 2(c). The cone-shaped Co particles have been examined by XRD and AES (Figs. 3 and 4). Well-distributed conic particles (70–200 nm) were embedded in the Si substrate. Figure 2(d) illustrates the ends of CNTs without catalytic particles, after they had been removed from Si substrate. Consequently, Figs. 2(a)–2(d) shown a typical base growth mode. The growth mechanism of CNTs is very similar to that suggested by other research groups,[11] in whose work graphite layers generated by CVD on catalytic particles were transformed into nanotubes that enclosed those the catalytic particles.[12] Various methods, including spin coating of a metal precursor and the sputtering of metal film have been used to derive a uniform distribution of catalytic particles to grow CNTs on a Si substrate. Generally, the deposited metal film is pretreated by H_2 or NH_3 plasma to remove oxide from the surface, forming clear and small metallic particles examined by plasma treatment. Figure 3 plots the XRD patterns of the Co-deposited Si substrate after *being* treated with H_2 plasma. The figure shows that $CoSi_2$ forms instead of CoSi formation. The latter is an intermetallic compound formed during annealing at high temperature ($>600\,^\circ$C) in the Co/Si system. Cobalt silicide has recently emerged as a preferred choice for use as a contact and interconnect material in microelectronics, because it has low resistivity (10–15 $\mu\Omega$) and excellent chemical stability. Moreover, in the upper spectrum of Fig. 3, Co metal is

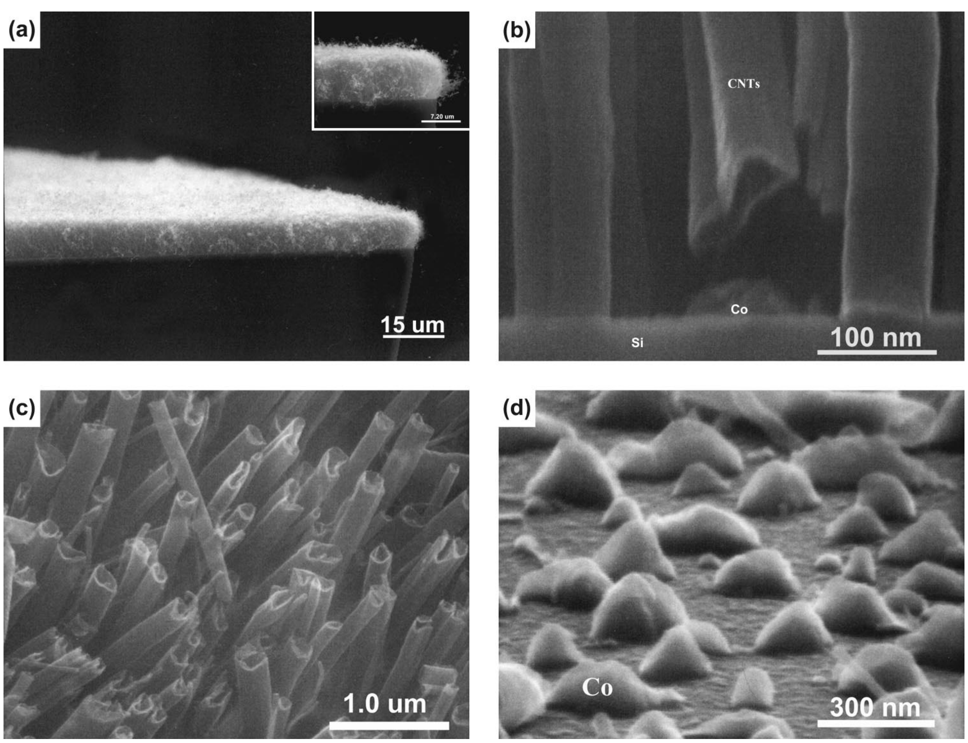

FIG. 2. SEM morphologies of CNTs grown without a SiO_2 barrier layer: (a) well aligned CNTs perpendicular to the substrate over a large area; (b) bottom of CNTs separated from Si and catalytic particles; (c) ends of CNTs without catalytic particles, removed from the Si substrate, and (d) cone-shaped catalytic particle embedded in the Si substrate.

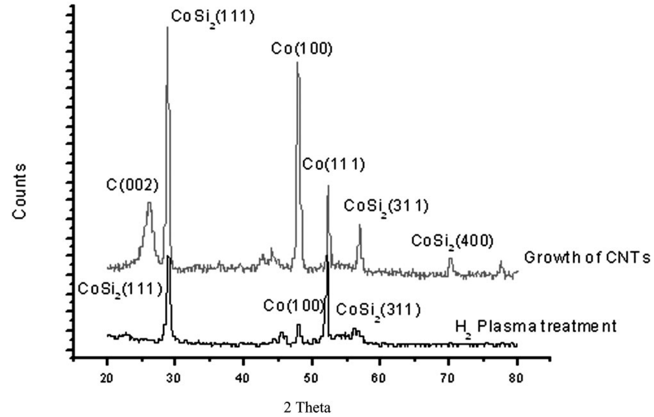

FIG. 3. XRD patterns of the base-growth sample under various conditions; (a) flowing H_2 plasma pretreatment, and (b) after growth of CNTs.

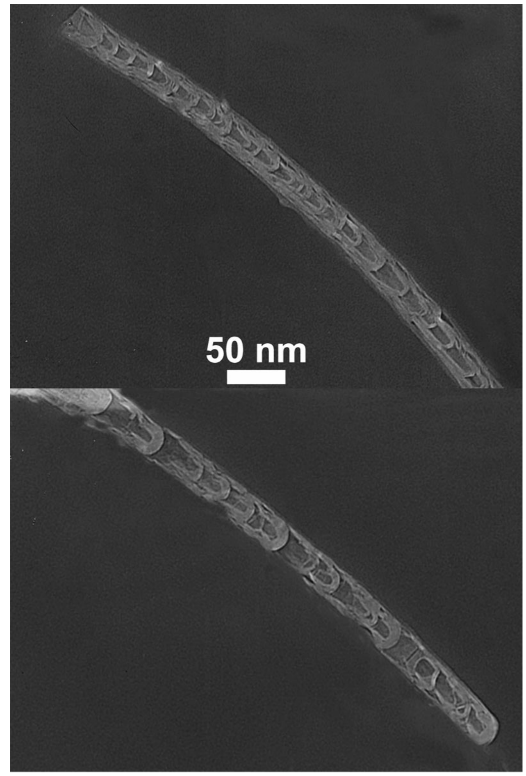

FIG. 5. TEM morphologies of no evident catalytic particles in CNTs ends.

found after CNTs are grown, and in the growth of CNTs, the discrete $CoSi_2$ layers seem to grow into the Si substrate below the continuous $CoSi_2$ layer, reducing the concentration of Co, according to a depth of the AES profile plotted in Fig. 4. Figure 5(a) presents bamboo-like multiwalled CNTs (MWCNTs) microstructures, which are similar to those observed by other research groups.[12] The diameter of the MWCNTs is around 90 nm, and the root and tips of CNTs are opened and closed, respectively. Catalytic particles are fixed on the substrate; implying that Co particles easily form the silicide.[13–15] Aligned CNTs, as presented in Fig. 6(a) are the glue used in preparing the cross-section TEM specimen. The triangular cobalt silicide ($CoSi_x$) is formed by the reaction between cobalt particles and Si during the growth process. Moreover, Fig. 6(a) clearly displays the interfaces between Co particles and the Si substrate. The Co diffuses into the Si substrate to form cobalt silicide with a facet interface. This reaction is believed to explain the strengthening of the adhesion between the Co catalyst and the substrate by silicide formation which would explain why the metal catalysts adhere strongly to the substrate during the growth of CNTs. The inset in Fig. 6(a) is highly magnified; it clearly presents Co particles and $CoSi_x$. The interfacial reaction between CNTs/Co and the Si substrate were examined, showing base-growth mode. Figures 6(b) and 6(c) show selected area diffraction (SAD) patterns and the numbers refer to different areas of diffraction, as shown in the inset in Fig. 6(a). Figure 6(b) presents the SAD (zone=[01-1]) pattern of Co catalytic particles together with CNTs, which indicates that the diffuse (002) diffraction spots of CNT are all in directions

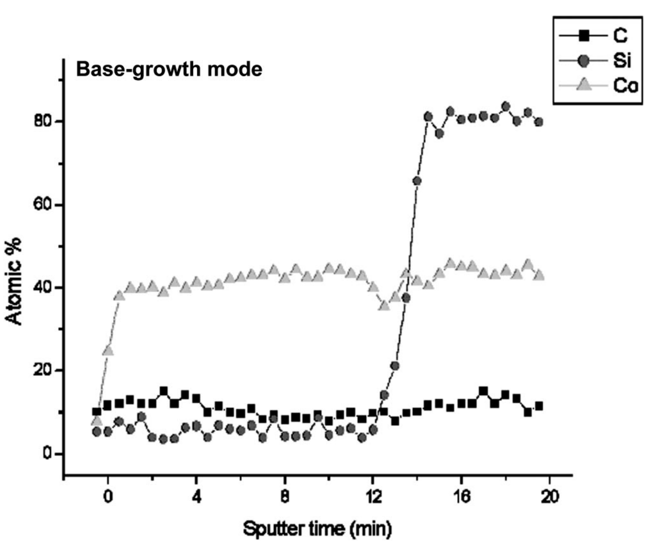

FIG. 4. AES depth profile of base-growth sample after growth of CNTs.

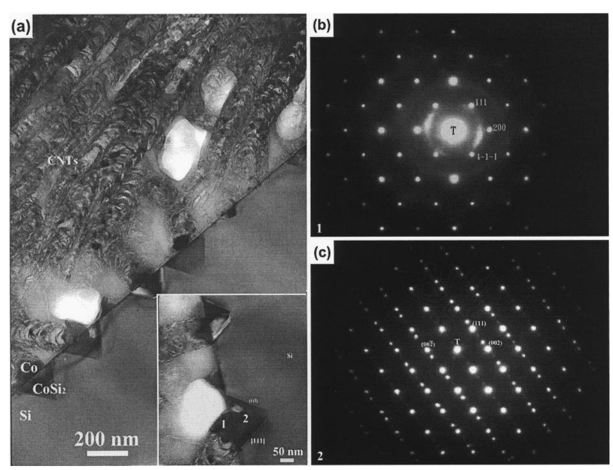

FIG. 6. Cross-sectional TEM images of (a) interfacial region of CNTs/Co/Si. Bamboo-shaped CNTs were clearly grown from a Co nanoparticle; (b) SAD pattern around the CNTs/Co interface, and (c) SAD pattern around the triangular $CoSi_2$/Si interface.

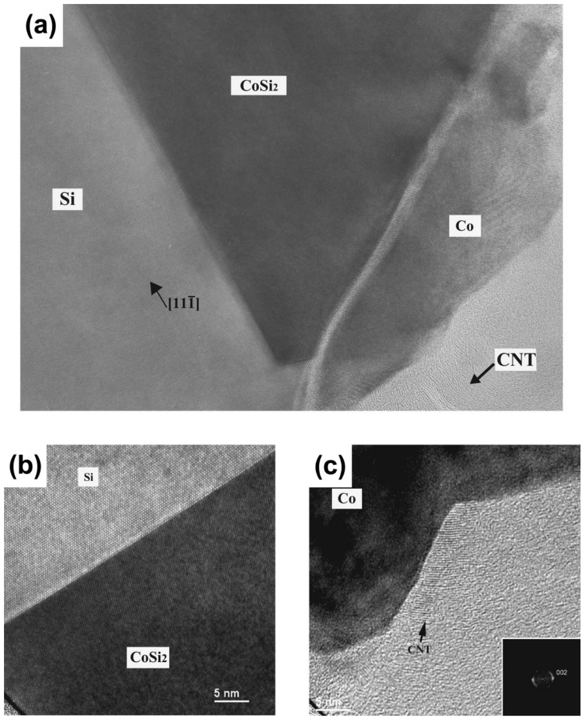

FIG. 7. HRTEM images of (a) interfacial region of $Co/CoSi_2/Si$ and (b) interfacial region of $CoSi_2/Si$; (c) HRTEM lattice image of the interface region, showing MWCNTs grown from a Co nanoparticle.

between Co (200) and Co (1-1-1). Figure 6(c) shows the SAD pattern of triangular $CoSi_2$ with the Si substrate and the zone axis [01-1]. The diffracted spots of (200) from $CoSi_2$ and Si coincide with each other, implying that a fully coherent relationships (A-type interface) exist between the orientation of $CoSi_2$ and that of Si.[16] Clearly, a triangular $CoSi_2$ layer with {111} and (100) facets is locally formed in the Si substrate. The nucleated $CoSi_2$ may be grown on a Si substrate with both {111} and (100) planes at the $CoSi_2/Si$ interface because the {111} interfacial energy of $CoSi_2$ is lower than the (100) interfacial energy. However, the precise behavior associated with epitaxial growth from amorphous carbonic cobalt is not yet fully understood, and warrants further study with reference to the potential applications in ultralarge scale integration.

A high-resolution TEM (HRTEM) micrograph along the ⟨100⟩ zone axis is obtained to assess the coherency of the CNTs, $CoSi_2$, and Si layer. Figure 7(a) presents a lattice structure image. An epitaxial (100) $CoSi_2$ layer with a small {111}-faceted interface is formed on the (100) substrate with a sharp silicide–silicon interface. Figure 7(b) shows a sharp silicide–silicon interface, clearly demonstrating the presence of an epitaxial layer. Several studies have found that the close lattice match between the $CoSi_2$ and Si crystal matrices, which exhibits only a ~1.2% lattice mismatch, enables the epitaxial growth of $CoSi_2$ on Si (100).[17] The epitaxial $CoSi_2$ on Si {111} exhibits coherence. Figure 7(c) presents a lattice image of Co particles and CNTs, and the inset in Fig. 7(c) shows the fast Fourier transform image of a (002) graphite layer of CNTs. Clearly, the graphite lattice grows from the

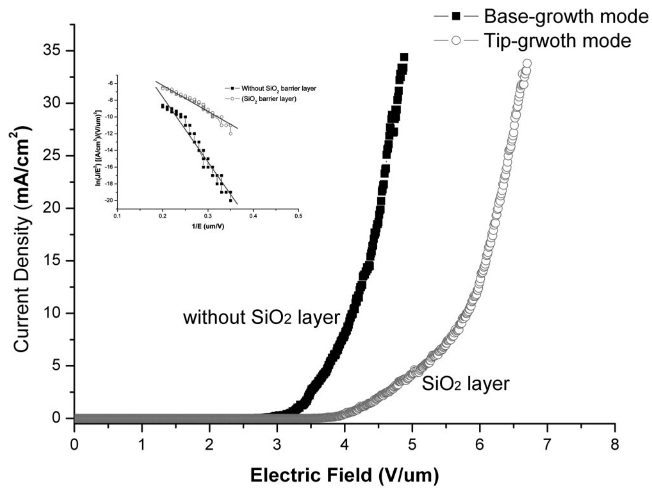

FIG. 8. Typical field emission $J-E$ curves of the vertically aligned tip-grown CNTs and of base-grown CNTs.

Co particles. All the evidencesupports the complete matching of the lattice across the interface, implying that the $CoSi_2$ layer is fully coherent with the Si substrate. Therefore, a $CoSi_2$ layer can be said to be epitaxially grown on a (100) Si substrate during the growth of CNTs, without an intermediate layer.

The catalysts usually remain at the tips of CNTs grown using plasma-enhanced CVD. However, in this work, the base-growth mechanism was observed and $CoSi_2$ was found to pin the CNTs into the Si substrate. This mechanism is supposed to be able to solve the conductive and adhesive problems in relation of the CNT–FED, in which the CNTs are easily pulled from the cathode toward the anode when applied high current. Figure 8 plots the emission current density curves of these base-grown CNT arrays, and compares them to the curves obtained from another tip-grown sample; the CNTs with diameters of 5 nm are well-aligned on the Si substrate and the Co particles are present at the tips of CNTs. Further details of the tip-grown CNTs array will be discussed in another article.[18] The turn-on voltage is 2.2 V/μm [linear limit of the Fowler–Nordheim (F–N) curve] and the maximum emission current density is 40 mA/cm^2 at 4.9 V/um, results that are sufficient for FED. The inset in Fig. 8 shows a good linear fit, implying that the emission current of both samples exhibits F–N behavior but with different slopes. According to the F–N equation, $J \propto (E^2/\phi)\exp(-B\phi^{3/2}/\beta E)$ with $B = 6.83 \times 10^9$ (VeVm^{-1}), the field enhancement factor (β) can be calculated from the slope of F–N curve, provided that the work function of the carbon nanotube CNTs is 5 eV, the same as for graphite. In this study, the field enhancement factor (β) of this bottom-growth carbon nanotube is 1530, which is much higher than that obtained from the tip-growth CNTs array ($\beta = 800$) obtained from Fig. 8. Some factors, such as the diameters of the CNTs and the work function of the prepared emitter used for field emission effect, implying that the Co catalyst at the tips of CNTs, although having a small diameter. According to numerous reports, the metal tip absorbs the residual gas in the vacuum chamber, increasing the work function of the tip.

IV. CONCLUSIONS

Aligned CNTs are grown by MPECVD in a Si substrate on which Co had been deposited. Interdiffusion between Co and the Si substrate strongly affect the growth characteristics and the F–E properties of CNT arrays. Cobalt silicides are shown to be formed with a full coherent interface with the Si substrate. The presence of the conical Co particles is also shown to be critical in growing aligned CNTs; the base-growth mode is demonstrated for the formation of CNTs in this work. Furthermore, the presence of the catalytic particles at the tips of the CNTs is detrimental to field emission applications. The CNTs onto whose $CoSi_2$ is pinned on Si substrate exhibit favorable emission characteristics; the F–N plots show highly enhanced field factors, implying that such an array of CNTs are important in FED.

ACKNOWLEDGMENTS

The authors would like to thank the Industrial Technology Research Institute (Contract Nos. A321XS9410 and A311XS31E1), the National Science Council (Contract Nos. NSC90-2216-E-009-034, NSC90-2216-E-009-035, and NSC90-2216-E-009-040) and the Ministry of Education of Taiwan (Contract No. MOE89-E-FA06-1-4) for financially supporting this research. Mao-Lin Huang of the Department of Materials Science and Engineering, National Tsing Hua Univerity is appreciated for preparing the HRTEM specimens.

[1] S. Iijima, Nature (London) **354**, 56 (1991).
[2] L. Kouwenhoven, Science **275**, 1896 (1997).
[3] M. Bockrath, D. H. Cobden, P. L. McEuen, N. G. Chopra, A. Zettl, A. Thess, and R. E. Smalley, Science **275**, 1922 (1997).
[4] J. H. Hafner, C. L. Cheung, and C. M. Lieber, Nature (London) **398**, 761 (1999).
[5] A. G. Rinzler, J. H. Hafner, P. Nikolaev, L. Lou, S. G. Kim, D. Tomanek, D. Colbert, and R. E. Smalley, Science **269**, 1550 (1995).
[6] W. B. Choi *et al.*, Appl. Phys. Lett. **75**, 3129 (1999).
[7] T. Arcos, F. Vonau, M. G. Garnier, V. Thommen, H.-G. Boyen, and P. Oelhafen, Appl. Phys. Lett. **80**, 2383 (2002).
[8] L. P. Biro *et al.*, Appl. Phys. Lett. **76**, 706 (2000).
[9] M. Chhowalla, K. B. K. Teo, C. Ducati, N. L. Rupesinghe, and G. A. J. Amaratunga, J. Appl. Phys. **90**, 5308 (2001).
[10] H. S. Rhee, T. W. Jang, and B. T. Ahn, Appl. Phys. Lett. **74**, 1003 (1999).
[11] Z. F. Ren, Z. P. Huang, J. W. Xu, J. H. Wang, P. Bush, M. P. Siegal, and P. N. Provencio, Science **282**, 1105 (1998).
[12] C. J. Lee and J. Park, Appl. Phys. Lett. **77**, 3397 (2000).
[13] H. S. Rhee, B. T. Anh, and D. K. Sohn, J. Appl. Phys. **86**, 3452 (1999).
[14] Y. Roichman, A. Berner, R. Brener, C. Cytermann, D. Shilo, E. Zolotoyabko, and M. Eizenberg, J. Appl. Phys. **87**, 3306 (2000).
[15] G. B. Kim, H. K. Baik, and S. M. Lee, Appl. Phys. Lett. **69**, 3498 (1996).
[16] A. Alberti and E. Rimini, Appl. Phys. Lett. **75**, 2924 (1999).
[17] N. G. Einspruch and G. B. Larrabee, *VLSI Electronic: Microstructure Science* (Academic, New York, 1983), Vol. 6, p. 330.
[18] C. M. Hsu, C. H. Lin, H. J. Lai, and C. T. Kuo, Thin Solid Films (in press).